Film-forming amines as corrosion inhibitors: a state-of-the-art review

Deni Jero, Nicolas Caussé, Nadine Pébère

npj | materials degradation

Review

Published in partnership with CSCP and USTB

https://doi.org/10.1038/s41529-024-00523-0

Film-forming amines as corrosion inhibitors: a state-of-the-art review

Deni Jero[1,2] ✉, Nicolas Caussé[1] ✉ & Nadine Pébère[1] ✉

This review summarizes the use of film-forming amines (FFAs) for corrosion protection in water/steam industrial circuits, focusing on carbon steel. It discusses industrial feedback on FFAs' benefits and challenges, alongside experimental methods for studying their inhibition and structural properties. Key research areas include FFAs' corrosion inhibition mechanisms, adsorption kinetics, and layer structures. The review also identifies knowledge gaps and suggests future research directions to deepen the understanding of FFAs.

Cycling operations, including startups, shutdowns, and layups/maintenance introduce corrosion risks and mechanical stresses to water/steam circuits, ranging from boilers to pressurized water reactors in nuclear plants. To address these challenges, film-forming amines (FFAs) are employed as corrosion inhibitors in neutral and alkaline environments to protect water/steam circuits, which are primarily composed of carbon steel. Research dating back to 1960 by Fujii and Aramaki[1], demonstrated the ability of FFAs to inhibit the corrosion of carbon steels in seawater. The objectives of FFA treatment include limiting corrosion during continuous operation/shutdown periods and minimizing the transport of corrosion products. Technical guidance documents from the International Association for the Properties of Water and Steam (IAPWS) offer recommendations for the application of FFAs in industrial plants. Furthermore, annual international conferences aim to foster collaboration between industrial users of film-forming substances (FFS), including FFAs, and academic researchers to further promote research. The last FFS conference was held in 2024, in Prato, Italy. This initiative seeks to mitigate application risks, reduce failures and enhance the efficiency of FFS applications. This review focuses on the current state of knowledge regarding FFAs, covering various research aspects such as inhibition and adsorption mechanisms, adsorption kinetics, and the molecular structure of FFAs layers. A significant challenge in this field is characterizing these thin organic layers on rough and corrodible surfaces under industrial conditions. To address this, a dedicated section discusses the experimental approaches used to analyze FFAs, including their advantages and limitations. Lastly, the review identifies gaps in the fundamental understanding of FFAs and provides recommendations for future research to enhance the understanding of their mode of action and improve their industrial application.

Film-forming amines as corrosion inhibitors

The general formula of film-forming amines is as follows:

$$R_1 - [-NH - R_2 -]_n - NH_2 \quad (1)$$

with R_1 being an aliphatic hydrocarbon chain containing between 8 and 22 carbon atoms, R_2 being a shorter hydrocarbon chain with 1 to 4 carbon atoms, and n being an integer ranging from 0 to 7[2]. Film-forming amines adsorb to metal surfaces through their polar amine group, while their apolar hydrocarbon chain establishes a protective layer, effectively isolating the metal from the corrosive environment. Commercially available film-forming amines include N-oleyl-1,3-propanediamine (OLDA) and octadecylamine (ODA). The chemical structures of these molecules are presented in Fig. 1.

These two molecules are characterized by very limited solubility in water at room temperature, and their solubility increases with increasing temperature[2]. However, there is no data available on the literature on FFAs solubility in water. FFAs are soluble in organic solvents, such as chloroform or benzene[3]. In water/steam circuits, FFAs are injected in the form of a salt or emulsions. Notable commercial formulations featuring OLDA include ODYVAP and Cetamine®, supplied by ODYSSEE Environnement and Kurita Water Industries Ltd., respectively. A widely used formulation incorporating ODA is ODACON®, manufactured by REICON. Other formulations such as FINEAMIN, HELAMIN, and Steamate PAS should be mentioned. The confidential nature of the exact composition of these commercial formulations complicates the comparison of their behavior across different studies.

ODA has a theoretical pK_a value of 10.6 at 25 °C, while OLDA possesses two distinct pK_a values, 10.6 and 8.4 at 25 °C, corresponding to the primary and secondary amine groups, respectively. Like all amines, FFAs are believed to increase the pH and conductivity of the solution. However, due

[1]CIRIMAT, Toulouse INP, Université Toulouse 3 Paul Sabatier, CNRS, Université de Toulouse, 4 allée Emile Monso—BP44362, Toulouse, cedex 4, France. [2]ODYSSEE Environnement-Service R&D, Belle Croix, Requeil, France. ✉e-mail: deni.jero@toulouse-inp.fr; nicolas.causse@toulouse-inp.fr; nadine.pebere@ensiacet.fr

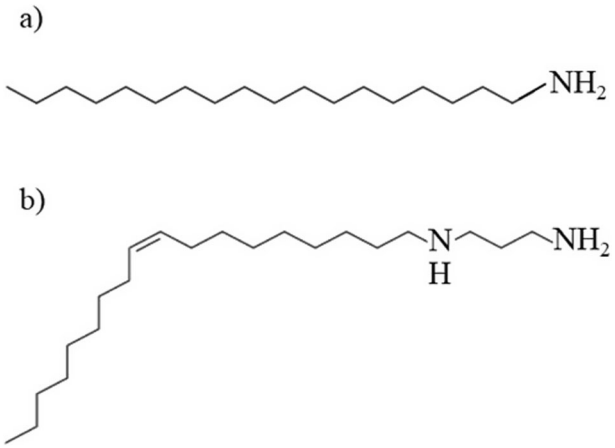

Fig. 1 | Film forming amines chemical structures. Chemical structures of (**a**) octadecylamine (ODA) ($C_{18}H_{39}N$) and (**b**) N-oleyl-1,3-propanediamine (OLDA) ($C_{21}H_{44}N_2$).

to the low concentration of FFAs required in industrial plants, their impact on pH and conductivity is negligible[4].

In the next section, several published feedback experiences on the use of these two FFAs in industrial installations (of all types) are presented.

Feedback on the use of film-forming amines in industrial plants

Industrial feedbacks underscore the multifaceted benefits of employing film-forming amines in water/steam plants. Overall, the FFA treatment minimizes general and localized corrosion, erosion-corrosion damage and stress-corrosion cracking of steels. It can be applied to different industrial systems, such as boilers and power plants and to different operational status startups, power operations, shutdowns and layups/maintenance. FFA treatment helps to clean circuits by removing bound deposits such as iron oxides from the surfaces. Moreover, this approach improves the heat transfer coefficient and it lowers the concentration of corrosion products in the feedwater. These points are discussed below.

In 2006, Chernyshev et al.[5] have reported the intermittent preservation of boiler surfaces, composed of steel by using an ODA emulsion at concentrations ranging from 200 mg kg^{-1} to 250 mg kg^{-1}. The application of ODA notably reduced corrosion processes, thereby reducing the vulnerability of the system. The adsorption of film-forming amines onto surfaces resulted in the liberation of anions, including chlorides present in oxide layers, due to their surfactant properties. In 2012, Topp et al.[6] have conducted a comparative study between an OLDA-based treatment and a phosphate treatment for steel surfaces. The authors observed a significant increase (80%) in the heat transfer coefficient for the OLDA treatment. Furthermore, they noted that the magnetite (Fe_3O_4)/hematite (Fe_2O_3) layers that formed after the OLDA treatment were more uniform and thinner than those formed after phosphate treatment. Similar conclusions were corroborated in 2015 by Ryzhenkov et al.[7] regarding the mitigation of corrosion processes during maintenance periods. Furthermore, an improved energy efficiency and a reduction in energy consumption within power plants were achieved by preventing deposits on boiler and turbine surfaces.

In 2016, Wagner et al.[8] have reported the preservation of an 800 MWe power plant using ODA in the form of ODACON®, which was administered in two injection phases. A visual inspection of the condenser after the initial phase revealed visibly cleaner surfaces than under pretreatment conditions. During the second injection phase, the conductivity values of the feedwater increased progressively, which, according to the authors, indicates effective surface protection and the removal of both deposits and chloride ions from the surface during the initial phase. In the same year, employing computational fluid dynamics (CFD) calculations, Rudolph et al.[9] have reported that film-forming amines contributed to a reduction in the quantity of corrosion product deposits in steam generators and reduced the size of the transported corrosion product particles. In 2017 and 2018, Smith et al.[10] and Hater et al.[11] have demonstrated the presence of OLDA molecules in Connah's Quay power plant using various techniques, such as residual concentration measurements and ex-situ X-ray photoelectron spectroscopy (XPS) analyses on coupons strategically positioned in different components of the plant and for temperatures up to 500 °C (vapor phase).

In 2021, Hoenig et al.[12] have quantified the technical and commercial advantages associated with film-forming amine treatments. The research study outcomes indicated a plant efficiency increase ranging from 0.3% to 1.1%, a reduction in water consumption, and a noteworthy 10–40% decrease in total heat exchanger costs due to reduced maintenance. In 2023, the efficiency of a commercial FFA (Helamin), as an alternative to an oxygen scavenger, in a high-pressure boiler has been confirmed by Rahman et al.[13] for an optimized concentration of 0.6 mg kg^{-1}. Iron and copper levels were reduced to trace levels. Physical examination of the FFAs exposed coupons revealed a uniform nonporous, dark grey film adhered to the surface, which appeared to be protective.

The initial injection of ODA into nuclear power plants was documented in the 1980s in Russia, but limited data are available, aside from indications that the injection outcomes were reportedly favorable. In 1988, in Armenia, two pressurized water reactors (WWER-440) were urgently shut down, and they were immediately conditioned with ODA (20 g kg^{-1}) in the form of an aqueous emulsion to protect the system[14]. The injection was conducted at nearly full power (420–430 MWe) for 100 h for Unit 1 and 160 h for Unit 2. Upon reopening in 1995, the water chemistry quality was deemed satisfactory. In 2011, AREVA GmbH executed the first ODA injection in a nuclear power plant at Almaraz (Unit 1, 1040 MWe) in Spain, preceding the planned annual shutdown[15]. The injection, was conducted in stages over 3 weeks, while the plant was operating at full power, following a protocol patented by Ramminger et al.[16]. No thermal degradation of ODA was observed at a temperature of 280 °C, and the favorable outcomes led to eight subsequent ODA applications between 2011 and 2016, preceding both units shutdown of the Almaraz plant (Units 1 and 2). In 2015, the Embalse power plant in Argentina underwent ODA conditioning administered by AREVA GmbH in preparation for a three-year shutdown[17].

However, several critical aspects of FFAs treatment should be mentioned related to the risks of overdosage, the thermal degradation of FFAs and the formation of low-molecular-weight organic acids that can have a negative effect and accelerate corrosion processes[2]. Special attention must be given to the risks of FFAs overdosage. According to IAWPS guidelines, FFAs should be gradually introduced into an industrial plant, starting with a lower dosage and increasing it to the target level to avoid oxide and deposit removal that could increase iron levels in feedwater. Dosage adjustments are based on preliminary studies and plant-specific feedback, typically ranging from 0.5 mg kg^{-1} to 10 mg kg^{-1}. A minimum period of 3–4 weeks is needed for this adjustment, varying by prior chemical treatments, materials, and operational mode. Overdosing can lead to precipitate formation and blocking of the pipelines, so dosage control is crucial. FFAs adsorption depends on metal surface area, temperature, and amine concentration, making it challenging to correlate dosage with free amine levels in water[2]. Other factors like solubility, thermal stability, and water/steam partitioning coefficient must also be monitored. The injection point is strategically chosen with a sufficiently high flow rate to prevent the accumulation of FFAs on the surface. If parameters deviate, the injection should be stopped, the system purged and the parameters stabilized once again[16]. Finally, FFAs molecules are reported to have an impact on reverse osmosis membranes and the ion-exchange resins. For example, Hasan et al.[18] have shown that ion-exchange resins are impacted by exposure to ODA by permanently reducing the mass transfer coefficient. The cationic resin capacity was reduced by 20%, and the anionic resin capacity was reduced by 37%.

Although the effectiveness of FFAs has been widely acknowledged[19] and they are extensively used in industrial circuits, there remains a significant lack of scientific understanding regarding the mechanisms through which FFAs influence iron oxide formation kinetics and provide corrosion protection. Additionally, the impact of physicochemical conditions on the

adsorption/desorption rates of FFAs, as well as on the structure and morphology of the layers they form, is still not fully understood. One of the primary reasons for the scarcity of fundamental research on FFAs is the difficulty in characterizing these molecules both in the feedwater and on metallic surfaces. The following section discusses the characterization methods employed in both industrial and laboratory settings to study FFAs.

Experimental approaches for studying the inhibition efficiencies and structural properties of FFA layers

In industrial settings, FFAs are primarily characterized through *ex post* analysis by estimating the residual FFAs concentration in the feedwater. In specific cases, coupons are introduced into the feedwater and analysed by ex situ observations.

The quantification of film-forming amines in industry is primarily performed by the complexation of these molecules with methyl orange or by the Bengalrose method described in 2011 by Stiller et al.[20]. The complex is extracted in organic solvents such as chloroform and dichloromethane. Other techniques, such as complexation with colored eosin[21], paper spray mass spectrometry (PS-MS)[22], or liquid chromatography coupled with high-resolution mass spectrometry (LC-HRMS)[23], have been described in the literature in 2015, 2016, and 2020, respectively. It is important to note that FFAs adsorb onto various polymer and glass surfaces[24], as well as onto measurement devices. As a result, the absolute concentration values of FFAs in solution are not known; only their temporal evolution can be evaluated. This adsorption also occurs on the surfaces of online instruments such as pH or conductivity electrodes, potentially compromising the accuracy of feedwater parameter measurements[25].

The presence of film-forming amines on metallic coupon surfaces is generally demonstrated by the water drop test. The adsorption of film-forming amines results in the formation of a hydrophobic surface, as indicated by the contact angle between the water droplet and the substrate exceeding 90°. A high contact angle value corresponds to a low surface wettability. Lee et al.[26] have measured a contact angle of 110 ± 2° on a high-chromium nickel alloy (alloy 690) surface in the presence of ODA as compared to 77 ± 1° on the same surface in absence of these molecules. These results indicate that the layer formed on the surface is more hydrophobic than the metallic surface. In industrial plants, this method is commonly used due to its rapid results. However, oxides found in water/steam circuits also exhibit hydrophobic characteristics[4], which makes this verification method somewhat unreliable for accurately detecting the presence of FFAs.

Under laboratory conditions, FFAs are studied in situ mostly by electrochemical techniques and ex situ by different surface analysis techniques. In situ electrochemical techniques such as electrochemical impedance spectroscopy (EIS) and polarization curves are generally used to study the inhibition efficiency of FFAs in different corrosive media. Recently, the FFAs layer thickness, adsorption kinetics and structural organization have also been investigated by EIS. Quartz crystal microbalance with dissipation monitoring (QCM-D) has been used to examine the amount of adsorbed FFAs on metallic surfaces. X-ray photoelectron spectroscopy (XPS), Raman spectroscopy, and infrared spectroscopy (IR) are generally used to characterize the presence of FFAs on surfaces but without truly investigating their adsorption mechanisms due to the limitations of the techniques. XPS is an extreme surface analysis technique and thus, highly sensitive to substrate roughness. This sensitivity makes it challenging to interpret the adsorption mechanisms of FFAs, particularly on rough and corrodible surfaces. IR and Raman spectroscopy, on the other hand, are sensitive to the amount of molecules i.e., they are not suitable for studying nanometer thin layers. An alternative to Raman spectroscopy is surface enhanced Raman spectroscopy (SERS), which enables the analysis of thin layers. However, this technique requires the use of nanostructured gold or silver surfaces to enhance the Raman signal. Several techniques, such as atomic force microscopy (AFM) and polarization modulation infrared reflection-absorption spectroscopy (PM-IRRAS) (detection limit below 10 nm), can be used to estimate thin-film thickness. These techniques are primarily performed ex situ (special setups can be implemented for in situ measurements) and are sensitive to surface roughness. Film-forming amines have been studied solely by AFM on model surfaces, such as gold or mica. Recently, PM-IRRAS has been used to study the OLDA layer thickness on mirror-polished steel surfaces. The use of these techniques to study FFAs is summarized in Table 1.

Table 1 | Surface characterization techniques used to study the inhibition efficiency, adsorption mechanisms, adsorption/desorption kinetics, and structure and morphology of the FFA layers

	Technique	References
Inhibition efficiency	EIS Polarization curves QCM-D	32,47,51,65,71
Adsorption mechanisms	XPS and Auger spectroscopy Raman spectroscopy IR	10,51,53,58–60,63,65,66
Adsorption kinetics	EIS	47,58
Structure and morphology of the layer	AFM PM-IRRAS EIS	42,47,53,58,62,63,65,68

In the next sections, the inhibition and structural properties of FFAs layers investigated by the aforementioned techniques will be discussed for different physicochemical conditions.

Corrosion inhibition properties of film-forming amines

This section aims to discuss the influence of concentration, temperature and chemical conditioning—particularly chloride ion concentration, pH, and dissolved oxygen, which are some of the most relevant parameters from an industrial perspective—on the mode of action and efficiency of film-forming amines.

Effects of the initial concentration

The concentration of FFAs in solution has a direct impact on the inhibition efficiency of these molecules. The optimal concentration of an organic inhibitor, given its surfactant nature, is often assimilated to the critical micellar concentration (CMC). There exists a Krafft temperature at which the CMC equals the solubility of the surfactant. The Krafft temperature is considered the minimum temperature for micelle formation. The CMC of a surfactant depends on several parameters, such as temperature, pH, ionic strength of the solution, and carbon chain length. According to Malik et al.[27], at concentrations below the CMC, minimal molecular adsorption occurs, resulting in partial anticorrosion protection. Beyond the CMC, the surface is covered by one or more layers, and corrosion protection is optimal. Any additional quantity added to the solution above the CMC leads to the formation of additional micelles in the solution and/or adsorbed layers, resulting in no notable improvement of the inhibition efficiency. There is no consensus in the literature, regarding the CMC of ODA or OLDA. The theoretical solubility of OLDA, also considered the CMC, in water ($pH_{25°C}$ = 7.0) was calculated to be 36 mg kg^{-1} as reported by the European Chemicals Agency (ECHA). However, Bohnsack[28] reported a CMC of 3-4 mg kg^{-1}. Mao et al.[29] measured an ODA CMC of 1.35 g L^{-1} using electrochemical techniques at 75 °C in an acidic solution ($pH_{25°C}$ = 4.2).

Other authors have studied the influence of FFAs concentration without mentioning the CMC but rather through the inhibition efficiency of the molecules, which is often assessed by electrochemical techniques. In 1981, Duprat et al.[30] have studied the influence of the concentration (375 mg kg^{-1}–1250 mg kg^{-1}) on the inhibition efficiency of a mixture of oleylamine and aminomethylphosphonic acid for XC35-type steel. A maximum inhibition efficiency of 82% was achieved at a concentration of 500 mg kg^{-1}, as determined by polarization curves in a 3% NaCl medium at room temperature. Beyond this value, the inhibition efficiency slightly decreased to 79%. In 2003, Rohani-Rad et al.[31] have investigated the effect of

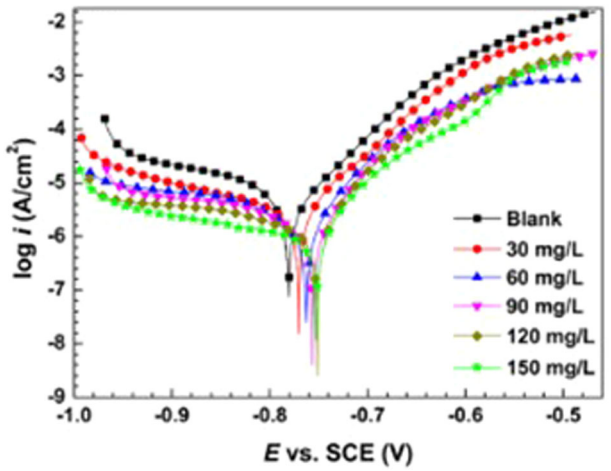

Fig. 2 | Influence of the FFAs concentration. Polarization curves for a carbon steel at 40 °C in the absence and presence of different concentrations of ODA. Adapted from ref. 33 with permission from Springer Nature© 2020.

ODA concentration on the surface of a heat exchanger (carbon steel) at 140 °C and $pH_{25°C}$ = 8.3 using potentiostatic measurements in a semi-industrial setup. In this study, the optimal ODA concentration was 0.2 mg kg^{-1}, and for higher concentrations (up to 3 mg kg^{-1}), the inhibition efficiency remained constant at 96%. In 2018, Pensini et al.[32] have reported the same adsorbed mass on a stainless steel surface for two OLDA concentrations, 25 mg kg^{-1} and 2500 mg kg^{-1}, resulting in the same corrosion inhibition efficiency. Analyses were conducted using QCM-D and EIS at 25 °C and $pH_{25°C}$ = 9.0 adjusted by NaOH. Similar conclusions were drawn in 2020 by Ma et al.[33]. The authors studied, through polarization curves, the influence of the concentration of ODA on the inhibition efficiency of carbon steel at 40 °C (Fig. 2). A maximum efficiency of 93% was achieved at a concentration of 120 mg kg^{-1}.

Effects of the chemical conditioning of the feedwater

In 1999, Bäßler et al.[34] studied the effect of ODA ($[ODA]_{initial}$ = 200 mg kg^{-1}) on chloride-induced localized corrosion (10^{-2} M NaCl) in a deaerated solution at $pH_{25°C}$ = 5.6 and at two temperatures (150 °C and 250 °C). Results obtained from electrochemical measurements emphasized that in the presence of ODA, a dense magnetite layer forms instead of a porous iron oxide layer.

In 2002, Banica et al.[35] have investigated the influence of an oxygen scavenger (hydrazine) and dissolved oxygen on the ODA efficiency ($[ODA]_{initial}$ = 50 mg kg^{-1}) for protecting a carbon steel at 200 °C and 250 °C. The authors concluded, based on polarization curves and quantification of the dissolved iron, that better efficiency was achieved for a solution conditioned with hydrazine at 350 mg kg^{-1}. The presence of oxygen (concentrations < 100 mg kg^{-1}) at the studied temperatures induced iron dissolution and thus, acidified the environment, preventing the formation of a protective oxide layer. Under these conditions, ODA did not form an effective film. ODA adsorption appeared to be more favorable in the presence of a protective oxide layer, as formed in the presence of hydrazine. Lee et al.[36] have found that the amount of magnetite deposited on filmed tubes with ODA decreased by approximately 58% compared to that on the as-received tube based on an increase in zeta potential and of the impedance modulus (EIS measurements) in the presence of ODA.

In 2020, De Seranno et al.[37] have studied the efficiency of OLDA ($[OLDA]_{initial}$ = 5 mg kg^{-1}) on a NiCrMoV alloy at 90 °C in an acidic environment adjusted with acetic acid. The authors concluded that although the presence of OLDA had no influence on the mechanisms of the electrochemical reactions, it seemed to disturb the accessibility of the active sites for redox reactions, decreasing both anodic dissolution and hydrogen embrittlement. In 2020, Weerakul et al.[38] have observed, through experiments in a recirculating water loop at 140 °C (corrosion-erosion phenomenon), that the addition of OLDA significantly reduced the corrosion rate of steel more than the addition of an alkalizing amine (cyclohexylamine (CHA)) and ammonium hydroxide. Injecting OLDA before CHA leads to better OLDA adsorption than adding an OLDA/CHA mixture. Measurements were conducted using an in situ electrical resistance probe, which allowed the metal mass loss to be monitored. The results were compared with OLDA concentration measurements using the Bengalrose method.

Effects of temperature

In 2000, Ge et al.[39] have determined the conditions required to achieve optimal protection of carbon steel. The highest polarization resistance values were obtained at a temperature of 220 °C, corresponding to a carbon steel treatment with 25 mg kg^{-1} of ODA (1 h) in a deaerated solution at $pH_{25°C}$ = 9.0–9.5 (adjusted with NaOH). In 2005, Bommersbach et al.[40] have studied the effect of a mixture of tertiary amine/carboxylic acid on steel protection as a function of temperature (20–80 °C). The exact formulation of the inhibitor was not provided. At a low concentration (0.5 m%.), the inhibition efficiency of the mixture decreased above 60 °C due to an acceleration of the steel corrosion kinetics. By increasing the concentration to 5 m%., the mixture remained effective up to 80 °C. In 2016 and 2017, Jäppinen et al.[41] have studied the influence of ODA on the corrosion protection of carbon steel in a deaerated environment at $pH_{25°C}$ = 9.2 adjusted by NH_3 at two temperatures (228 °C and 300 °C). The corrosion rate, determined by EIS and mass loss measurements, was reduced by a factor of two in the presence of ODA, at both temperatures. Adding ODA at the beginning of the experiment (bare steel surface) or after a preoxidation period of the steel did not change the results. In 2020, Baux et al.[42] have investigated the protective role of ODACON® in a deaerated environment in the presence of 1 mg kg^{-1} of hydrazine at $pH_{25°C}$ = 9.6 adjusted by ethanolamine and ammonia, for three temperatures: 120 °C, 220 °C, and 275 °C. Films were formed under the abovementioned conditions and analyzed at room temperature by EIS. After treatment with an ODA concentration of 2 mg kg^{-1} for 168 h, the film was detected at a temperature of 120 °C only. At 220 °C, it was necessary to increase the ODA concentration to 25 mg kg^{-1} and to reduce the treatment time to 2 h to confirm the presence of a film in the impedance spectra. Treatment of the steel with ODACON® (2 mg kg^{-1} of ODA) at 275 °C was carried out in the vapor phase. Considering the partition coefficient of ODA between the liquid and vapor phases, the ODA concentration was close to 6.5 mg kg^{-1} in the vapor phase, assuming minimal adsorption on the autoclave walls and no molecular degradation under these conditions. It was observed by impedance measurements that between 2 h and 24 h of treatment, the high-frequency response of the ODA film was missing. This was attributed to molecular degradation at this temperature, as confirmed by the measurement of the ODA concentration over time (Fig. 3), the analytical technique not being specified. The authors concluded that concentration, temperature, and treatment time are crucial parameters for ODA performance at high temperatures. Additionally, there was a "critical temperature" between 120 °C and 275 °C at which the efficiency decreased probably due to the degradation of ODA.

In 2020, Cuoq et al.[43] have monitored OLDA adsorption ($[OLDA]_{initial}$ = 7–8 mg kg^{-1}) on AISI 316 stainless steel over time and at various temperatures by determining the residual concentration in the solution (Bengalrose method). At 70 °C, the steady state, i.e., the stabilized OLDA concentration at 4 mg kg^{-1} was reached after 41 h, corresponding to an adsorption coefficient of 0.015 h^{-1}. The device was cooled to 44 °C by creating a thermal gradient between the solution and the device to simulate conditions in industrial installations. The residual OLDA concentration decreased until it stabilized after 42 h; the adsorption coefficient then became 1.5 h^{-1}, indicating a two-order-of-magnitude increase in adsorption. With an increase in temperature, OLDA desorption was observed. An additional experiment conducted by decreasing the temperature of the solution without the thermal gradient showed that the amount of adsorbed

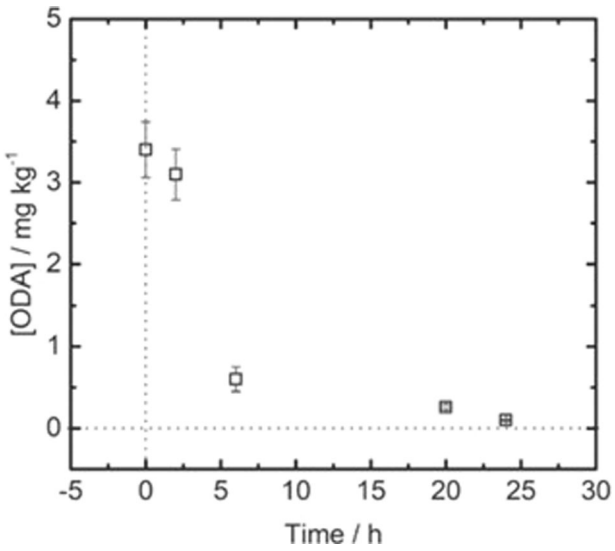

Fig. 3 | FFAs thermal degradation. ODA concentration in the liquid phase at 275 °C as a function of time. Adapted from ref. 42 with permission from IOP Publishing© 2020.

OLDA remained unchanged. The authors concluded that the significantly increased adsorption of OLDA was triggered by the positive surface charge created by the Seebeck effect due to the thermal gradient, leading to an enhanced driving force for OLDA adsorption. Finally, in 2021, Kuilya et al.[44] have reported that for an Incoloy-type alloy and an identical ODA concentration (20 mg kg^{-1}) in the liquid and vapor phases at 200 °C, better protection was achieved in the liquid phase, based on inhibition efficiencies values determined by EIS at room temperature.

Another important parameter to consider is the thermal decomposition of these molecules for which there is no consensus. According to Cao et al.[45], ODA appears to be stable up to 560 °C in the vapor phase, and the decomposition products do not contain organic acids that can decrease the pH of the environment and thus favor the dissolution of oxide layers. According to the IAPWS guidelines, ODA decomposes into CO_2(g), H_2(g), CH_4(g), and NH_3(g) at 450 °C, while OLDA is stable up to 300 °C without the production of organic acids. Other authors have reported decomposition temperatures between 85 °C and 350 °C, that are dependent on the treatment time. The decomposition products include shorter-chain amines, ammonium ions (NH_4^+), or small carboxylates such as the acetate ion CH_3COO^-. However, other parameters, such as the initial concentration of FFAs (up to 20 mg kg^{-1}), the pressure (varying from 3 MPa to 17 MPa) and the different components contained in industrial formulations, can influence FFAs thermal degradation as resumed in a recent review[46].

Various studies have demonstrated the efficiency of these molecules under a wide range of feedwater physicochemical conditions. However, most research remains comparative, and the underlying mechanisms are still not well understood. Additionally, these studies are rarely paired with analytical or surface analysis techniques that would link inhibition efficiency to the properties of FFAs in solution and, subsequently, to the structure of the layers formed on surfaces, partly due to the challenges in characterizing these molecules.

Film-forming amines adsorption mechanisms

The inhibition mechanisms of OLDA have been recently investigated in various corrosive media by polarization curves which are shown in Fig. 4[47].

Regardless of the medium, OLDA decreased the anodic and cathodic current densities minimizing the corrosion rate of the carbon steel. The molecules act as a mixed inhibitor; their adsorption blocks both the anodic and cathodic sites but does not alter the corrosion mechanisms in accordance with the results of De Seranno et al.[37].

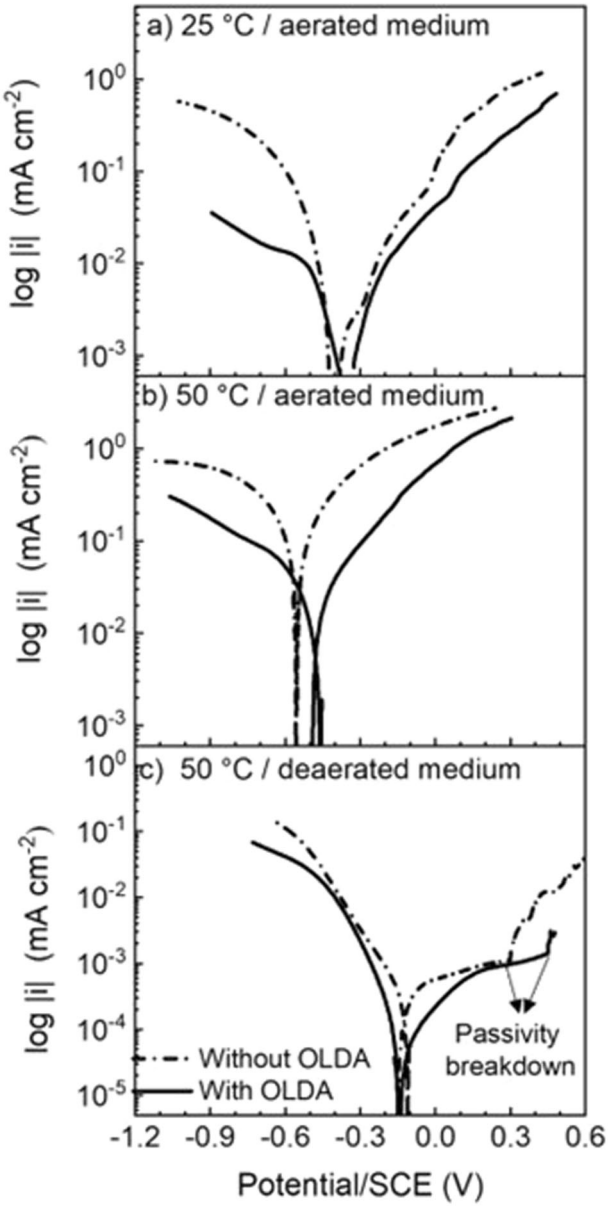

Fig. 4 | Influence of the corrosive medium on the OLDA inhibition mechanisms. Polarization curves for the carbon steel with and without OLDA (100 mg kg^{-1}) obtained after 140 min of immersion in different corrosive media: (**a**) 25 °C/aerated medium/$pH_{25°C}$ = 11.0/200 mg kg^{-1} NaCl; (**b**) 50 °C/aerated medium/$pH_{25°C}$ = 11.0/200 mg kg^{-1} NaCl; (**c**) 50 °C/deaerated medium/$pH_{25°C}$ = 11.0/26 mg kg^{-1} of diethylhydroxylamine (DEHA). Adapted from ref. 47 under the CC BY license© 2024.

The inhibition mechanisms of organic molecules are directly linked to their adsorption mechanisms[48]. The specificity of FFAs is attributed to the affinity of amine groups for metal surfaces and oxides. These molecules adsorb via their amine function(s) but their adsorption mechanisms and modification of the oxide growth have not been clearly identified.

In 1981, Duprat et al.[30] have proposed the mechanism schematically shown in Fig. 5, which illustrates the interaction between ethanolamine and iron hydroxides. The iron hydroxide layer is stabilized by Lewis interactions between iron and oxygen (oxygen acting as electron donor). The addition of the inhibitor led to the formation of chelates between the iron oxide layers and the nitrogen and oxygen atoms of the inhibitor. In addition, the molecules of the inhibitor formed hydrogen bonds. This mechanism was subsequently adopted to explain FFAs adsorption. However, this mechanism has not been experimentally verified.

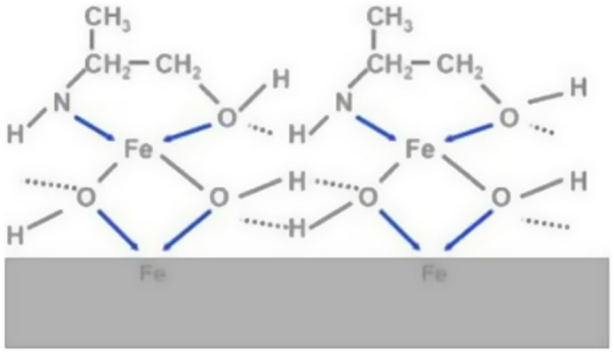

Fig. 5 | Schematic representation of the mechanism between ethanolamine and iron hydroxides. Adapted from ref. 30 with permission from Corrosion© 1981.

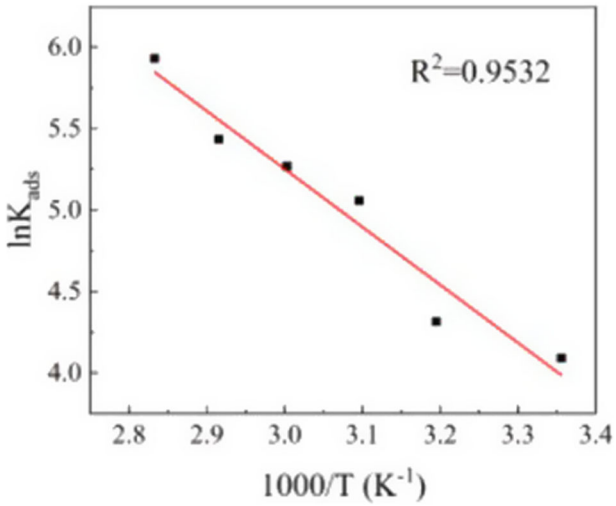

Fig. 6 | van't Hoff diagram of OLDA. Plot of $\ln(K_{ads})$ vs. 1000/T of the OLDA inhibitor. Adapted from ref. 52 with permission from Elsevier© 2021.

In 2003, Kumar et al.[49] have investigated the interactions between ODA molecules and gold nanoparticles. Two binding modes formed by complexation of the amine group with the gold surface were identified by combining XPS, nuclear magnetic resonance (NMR H^1), thermal gravimetric analysis (TGA) and IR analyses. The first binding mode involved protonated amine groups electrostatically complexed with $AuCl_4^-$ ions present on the surface of gold nanoparticles (Eq. 2). The formed species were stable up to 260 °C. The second binding mode corresponds to the $AuCl(RNH_2)$ complexes, which were stable up to 560 °C, as determined by TGA (Eq. 3).

$$\left[Au_n^0\left(AuCl_4^-\right)_m\right]_{(aq)} + mRNH_{3\,(org)}^+ \rightarrow \left[Au_n^0\left(AuCl_4^-\right)_m\right](RNH_3^+)_{m(org)} \quad (2)$$

$$\left[Au_n^0\left(AuCl_2^-\right)_m\right]_{(aq)} + mRNH_{3\,(org)}^+ \rightarrow Au_n^0\left[AuCl(RNH_2)\right]_{m(org)} + HCl \quad (3)$$

In 2010, Khodyrev et al.[50] have proposed that at low temperatures (40–80 °C), free valences (V) on the metal surface react with neutral ODA molecules according to the following radical reaction (Eq. 4).

$$V + C_{18}H_{37}NH_2 \rightarrow VC_{18}H_{37}NH + H^{\bullet} \quad (4)$$

The produced H• radical donates its electron either to the metal or to $VC_{18}H_{37}NH$, and the ODA adsorption cycle on the surface repeats. For temperatures above 100 °C and in the presence of a large number of OH• radicals (resulting from the oxidation of iron in an alkaline medium), the first step of the reaction is described below (Eq. 5).

$$OH^{\bullet} + C_{18}H_{37}NH_2 \rightarrow C_{18}H_{37}NH^{\bullet} + H_2O \quad (5)$$

The free radical $C_{18}H_{37}NH^{\bullet}$ can adsorb onto metallic surfaces, generating a new chemisorbed $VC_{18}H_{37}NH$ molecule and a new radical, i.e., a free valence (V). In 2016, Wagner et al.[8] have hypothesized that the adsorption/desorption equilibrium of FFAs on metallic surfaces depends on the temperature. According to the authors, for temperatures below 100 °C, physical bonds form *via* van der Waals forces, and for temperatures above 100 °C, chemical bonds form. However, no experimental confirmation has been provided. In 2019, Fan et al.[51] have studied the corrosion inhibition mechanisms of a supramolecular complex (CDOD) based on ODA (guest), considered hydrophobic, and β-cyclodextrin (host), considered hydrophilic, toward mild steel in condensate water ($pH_{25°C} = 5.8$, $\sigma_{25°C} = 110$ μS cm^{-1}). ODA was efficiently dissolved in the condensate water via the host compound and then it was subsequently released at the steel/electrolyte interface and assembled as a hydrophobic layer on the steel surface, as confirmed by contact angle measurements. Polarization curves showed that CDOD acted like as anodic-dominant mixed corrosion inhibitor. The activation enthalpy was found to be positive, which indicates an endothermic adsorption. The Gibbs free energy was near 40 kJ mol^{-1} representing a mixed type adsorption, including physisorption and predominant chemisorption. In this study, molecular dynamics (MD) simulation and quantum chemical calculation were also employed. MD simulations were performed in a weakly acidic environment at 308 K and in consideration of solvent effect. The simulations indicated that ODA adsorbed onto iron (111) surface at an inclined angle through its amine group. The calculated binding energy of 1862 kJ mol^{-1} reflected the efficient adsorption of the inhibitor. Quantum chemical calculations revealed that the distribution of the Highest Occupied Molecular Orbital (HOMO) and Lowest Unoccupied Molecular Orbital (LUMO) of ODA favored adsorption on the steel surface in a stereoscopic direction rather than parallel by the combined electron donor and acceptor. The HOMO and LUMO energies of −5.070 eV and −2.321 eV, respectively, suggested a strong inhibition effect similar to other reported amine derivatives for mild steel in acidic media. Additionally, the electron transfer fraction of 0.409 confirmed the significant tendency of ODA to interact with the steel surface through an electron-donating process.

In 2021, Jiang et al.[52] have determined the ΔG_{ads}^0 of the adsorbed OLDA on a carbon steel surface in a 37% HCl solution. Langmuir isotherms were plotted for different temperatures ranging from 25 °C to 80 °C. The surface coverage rate was assimilated to the inhibition efficiency determined by mass loss measurements. The obtained values of ΔG_{ads}^0 were negative indicating spontaneous sorption. As an absolute value, ΔG_{ads}^0 increased from 20 kJ mol^{-1} at 25 °C to 29 kJ mol^{-1} at 80 °C, indicating both physical and chemical interactions. Furthermore, by plotting the sorption constant against the inverse of temperature (van't Hoff diagram), as illustrated in Fig. 6, a positive value of enthalpy was obtained, suggesting endothermic adsorption in agreement with Fan et al.[51].

In 2022, Yoshioka et al.[53] have investigated the mechanisms of OLDA film formation on a copper surface at 150 °C by combining inductively coupled plasma atomic emission spectroscopy (ICP-AES), nuclear magnetic resonance (NMR) and infrared spectroscopy. The authors found a ratio of 1:6 between cuprous ions and OLDA molecules, and concluded that OLDA formed complexes with Cu ions by acting as a bidentate ligand.

In 2022 also, Genxian et al.[54] have found through focused ion beam (FIB) and transmission electrons microscopy (TEM) analyses that the ODA film formed on a preoxidized carbon steel surface was a multilayer. Based on the literature, such as the papers of Liu et al.[55] and Betova et al.[2], a schematic diagram of the multilayer adsorption model on the surface of preoxidized carbon steel was proposed by the authors (Fig. 7). The ODA molecules in the

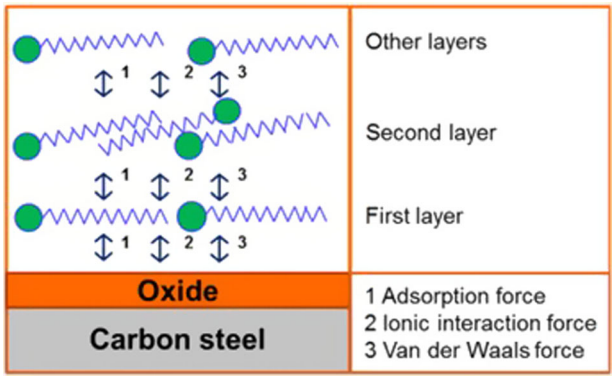

Fig. 7 | Schematic representation of the multilayer adsorption mechanisms of FFAs on a preoxidized carbon steel surface. Adapted from ref. 54 with permission from Elsevier© 2022.

first layer would be parallel to the surface of the oxide, meaning that both the amine group and alkyl group can be adsorbed on the surface. The second and third layers would interact by ionic and van der Waals forces. However, no experimental evidence was given to support these hypotheses.

Other authors have observed that the adsorption of corrosion inhibitors on iron oxides alters their growth and morphology. In 2012, Topp et al.[6] have studied the effect of OLDA on the growth of iron oxide layers at 196 °C. The authors found that the adsorption of the OLDA molecule did not prevent the formation of the oxide layer. However, analyses by confocal microscopy showed that the oxide layer was thinner and more uniform in the presence of OLDA. In 2012, Liu et al.[56] have studied the effect of ODA on the formation, morphology and magnetic properties of hydrothermally prepared iron oxide (α-Fe_2O_3). The adsorption of ODA on the iron oxide particles delayed their growth by the formation of smaller particles.

It is widely accepted that FFAs adsorb primarily through their amine groups, with various models proposed, including radical mechanisms, physisorption/chemisorption, and chelates/complexes. However, many of these proposed mechanisms lack experimental verification. To truly understand the mode of action of FFAs, it is crucial to investigate their adsorption mechanisms under the operational conditions of water/steam circuits. This is complicated by factors such as surface roughness, which limits the effectiveness of many surface analysis techniques. Molecular dynamics simulations offer a promising approach to studying adsorption mechanisms, yet they often fall short by not fully accounting for the complexity of real-world systems. Typically, these simulations analyze only a single plane lattice, while actual surfaces are composed of alloys and are subject to simultaneous corrosion processes.

Adsorption kinetics of film-forming amines

The influence of time on the adsorption and desorption of FFAs is a crucial parameter for improving injection protocols (frequency, concentration) for these molecules in water/steam circuits. However, this aspect has been studied very little in the literature, and if so, tests have been carried out by measuring the residual FFAs concentration rather than directly studying the surfaces. The inhibition properties of FFAs as well as the adsorption/desorption kinetics depend on the physicochemical conditions of the feedwater, such as concentration, pH, dissolved oxygen, temperature and flow velocity. The desorption kinetics also depend on the presence or absence of FFAs in the feedwater.

In 2015, Jack et al.[57] have reported the adsorption/desorption kinetics of OLDA at $pH_{25°C}$ = 9.2–9.3 in a stainless-steel circulation loop with a hot section at 140 °C. The residual OLDA concentration was determined by the Bengalrose method. The injection was performed continuously for a total duration of 1200 h. The adsorption and desorption kinetics were modeled by first-order constants. According to the authors, the studied kinetics corresponded to a labile layer (physisorbed) and not to a layer directly adsorbed on the steel surface. However, this hypothesis has not been

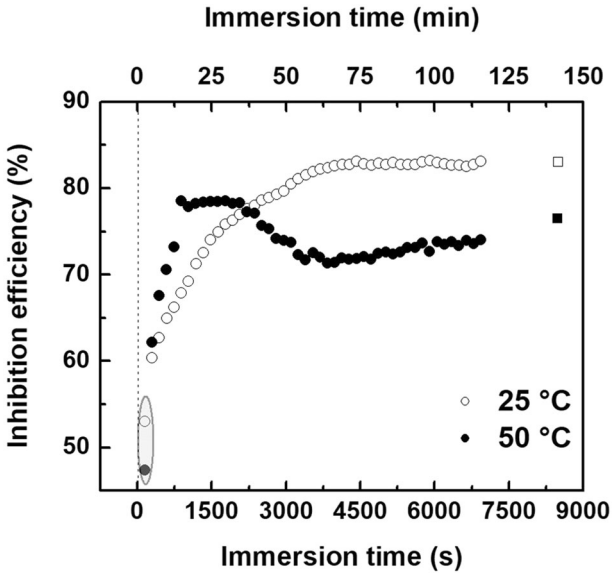

Fig. 8 | OLDA adsorption kinetics study. OLDA inhibition efficiency as a function of time determined from EIS measurements at 25 °C (○) and 50 °C (●) calculated for the following conditions: 100 mg kg^{-1} of OLDA, 200 mg kg^{-1} of NaCl, non-adjusted pH and aerated solution. Adapted from ref. 58 with permission from Elsevier© 2023.

confirmed. In 2017, Jäppinen et al.[41] studied the influence of exposure time to ODA ($[ODA]_{initial}$ = 20 mg kg^{-1}) at 228 °C and $pH_{25°C}$ = 9.8 (adjusted with ammonia) on carbon steel. The authors observed a slight but continuous increase in polarization resistance, as determined by EIS, over 71 h.

Recently, the OLDA adsorption kinetics on carbon steel were investigated by EIS for different physicochemical conditions[58]. At a concentration of 100 mg kg^{-1}, the inhibition efficiency was approximately 50% (Fig. 8) after 2 min of immersion which suggested that the OLDA molecules adsorbed immediately on the steel surface. OLDA kinetics were also followed by monitoring the capacitance variation over immersion time extracted from the high frequency region in impedance spectra (Fig. 9). When corrosion processes were limited by the chemical conditioning of the solution, the OLDA adsorption kinetics stabilized within the first 30 min of immersion. In deaerated media, OLDA adsorption kinetics were found to be independent of temperature (25–50 °C) (Fig. 9a). However, when steel corrosion and OLDA adsorption occurred simultaneously, the steady state was slower to establish, likely due to concurrent OLDA adsorption onto corrosion products during their formation (Fig. 9b).

Further investigation into the adsorption kinetics of FFAs is necessary, with a particular focus on parameters such as FFAs concentration in solution and elevated temperatures. It is crucial to pair analytical and surface techniques to effectively link the adsorption kinetics with frequency injection and dosage of FFAs. Additionally, conducting experiments in water circulating loops could provide valuable insights, as these setups can more accurately replicate the flow regimes encountered in water/steam circuits.

Thickness and molecular structure of the film-forming amine layers

In the present section, several physical models of the molecular structure of FFAs layers are discussed.

In 1998, Takahashi et al.[59] have studied the adsorption of Langmuir-Blodgett (LB) films of ODA transferred from a chloroform solution to an alkaline phase surface (distilled water with NaOH at a $pH_{25°C}$ = 10.1–10.5). Using FTIR analyses, they concluded that the ODA carbon chains in a "*trans zig-zag*" conformation formed an angle of 4.5° with respect to the surface. In 2005, Dai et al.[60] have investigated the structural properties of Langmuir–Blodgett films of ODA on Ag particles using SERS. The ODA monolayer was partially ordered and in a "liquid-crystalline" state due to strong interactions between the amine group of ODA and the Ag

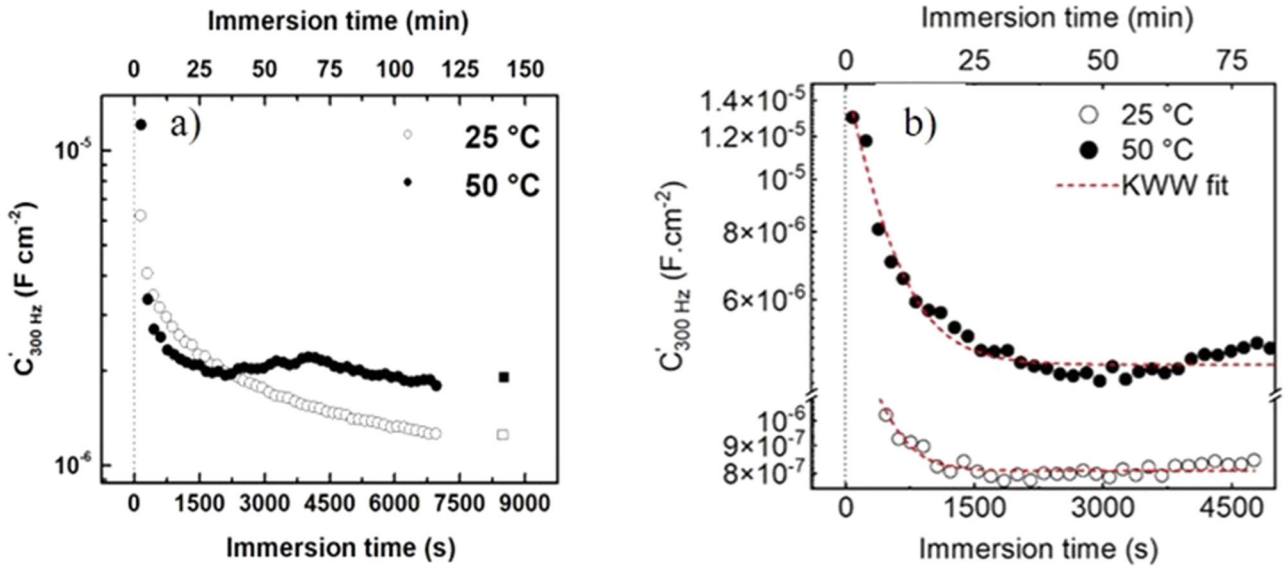

Fig. 9 | Influence of the corrosive medium on the OLDA adsorption kinetics studied by EIS. Capacitance variation as a function of immersion time at 25 °C (○) and 50 °C (●) for the carbon steel immersed into (**a**) an aerated medium of 100 mg kg^{-1} OLDA/200 mg kg^{-1} NaCl/non-adjusted pH (adapted from ref. 58 with permission from Elsevier © 2023) and (**b**) a deaerated medium of 100 mg kg^{-1} OLDA/26 mg kg^{-1} DEHA/pH$_{25°C}$ = 11.0 (adapted from ref. 47 under the CC BY license© 2024).

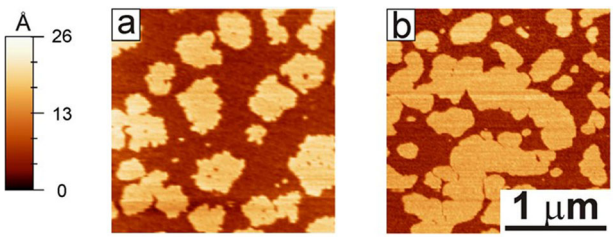

Fig. 10 | ODA molecular structure. AFM images of ODA islands on mica surface prepared from a 15 mM chloroform solution: (**a**) after 2 h and (**b**) after 7 days in contact with air. Adapted from ref. 62 with permission from American Chemical Society© 2012.

nanoparticles. In 2010, Patil et al.[61] have determined, by AFM, a thickness of an ODA film formed on mica equal to 20 nm, suggesting a multilayer structure (the length of an ODA molecule is approximately 2 nm). Oviedo et al.[62] and Campen et al.[63] in 2012 and 2015, respectively, have investigated the structure of ODA on a mica surface using AFM and FTIR. In both studies, topographical characterizations of the surface showed the formation of ODA islands with thicknesses between 1.5 and 1.7 nm, as shown in Fig. 10[62]. Oviedo et al. determined a chain tilt angle of ODA with respect to the surface of 46° after 2 h of layer preparation and 58° after 7 days of preparation. This difference was attributed to a "ripening" effect due to the protonation of the amine group with humid air. Campen et al. suggested that the islands formed by the inclined ODA molecules are held together by van der Waals forces between adjacent carbon chains. In addition to the FFAs adsorption, several authors have observed the formation of carbamate groups (-NH-COO$^-$) on mica surfaces[62,64]. The presence of the carbamate group was attributed to the rapid reaction between the ODA molecules and dissolved CO_2.

In 2017, Jäppinen et al.[41] have investigated the thickness of the ODA layer on carbon steel under conditions similar to those used in secondary circuits (pH$_{25°C}$ = 9.5 adjusted with NH_3). Using ex situ glow discharge mass spectrometry (GDMS), the authors estimated a thickness of 40 nm at 228 °C, 120 nm at 300 °C when ODA was added after 130 h (for a total duration of 151 h), and 160 nm when ODA was added from the beginning of the test (for a total duration of 160 h). In 2018, Baux et al.[65] have estimated the thickness of ODA films formed on a carbon steel surface by EIS. For ODA films formed for 30 min at 80 °C, pH$_{25°C}$ = 10.0, and analyzed by EIS at room temperature, the estimated thickness varied between 12 and 22 nm. The same thickness (20 nm) was determined by Baux et al.[42] for the ODA layer formed on the magnetite surface at 120 °C (168 h immersion) and 220 °C (2 h immersion) for pH$_{25°C}$ = 9.6–9.8 (adjusted with NH_3 and ethanolamine) and analyzed by EIS at room temperature. These results suggested that the ODA film thicknesses were independent of the physicochemical conditions, contradicting the ex situ results of Jäppinen et al.[41]. However, it must be noted that the thicknesses were assessed under different conditions and surface techniques, so direct comparisons cannot be made. In 2022, Yoshioka et al.[53] have studied the formation of an OLDA barrier at 150 °C on a copper surface. By mapping the surface with infrared microscopy, the authors noted the heterogeneous distribution and thickness of the OLDA layer, as shown in Fig. 11. Moreover, the orientation of the OLDA molecules depended on the thickness. Indeed, for molecules directly adsorbed on the surface, the carbon chains were organized, while with increasing thickness, they became disordered. According to the authors, Cu-OLDA complexes may induce the formation of a "polymer" network.

In 2007, Liao et al.[66] have investigated the surface of iron treated with ODA ([ODA]$_{initial}$ = 25 mg kg^{-1}) at 220 °C for 1 h using Auger spectroscopy, measuring the etching rate of Fe, C, and O. The authors concluded that the structure of the formed barrier consisted of an external layer of ODA, an intermediate layer containing both ODA and iron oxides, and an internal layer of iron oxide. However, the authors did not present nitrogen signal spectra, which are generally considered evidence of amine adsorption on the surface. In 2015, Mao et al.[29], based on a theoretical model that allowed to fit EIS diagrams obtained at 75 °C in a deaerated solution of acetic acid, proposed that ODA molecules combined with corrosion products to form "a mixed and compact external layer of inhibitor/oxide". In 2020, Liu et al.[55] have shown through ex situ scanning electronic microscopy (SEM), TEM and in situ EIS measurements that the ODA thickness increased with increasing ODA concentration in an anaerobic alkaline solution at 40 °C. The authors proposed multilayer adsorption mechanisms for ODA molecules on a carbon steel surface. The number of layers was calculated by Materials Studio simulations and was found to vary from 49 to 126 for concentrations varying from 1 mg kg^{-1} to 50 mg kg^{-1}, respectively.

Recently, the OLDA layer thicknesses on carbon steel surfaces have been estimated by PM-IRRAS as a function of time for two extreme cases; first in an aerated medium, 200 mg kg^{-1} NaCl and non-adjusted pH at 25 °C (Fig. 12a) and 50 °C[58], second in a deaerated medium, without any chloride ions in the solution and pH$_{25°C}$ = 11.0 for three temperatures 25 °C, 50 °C

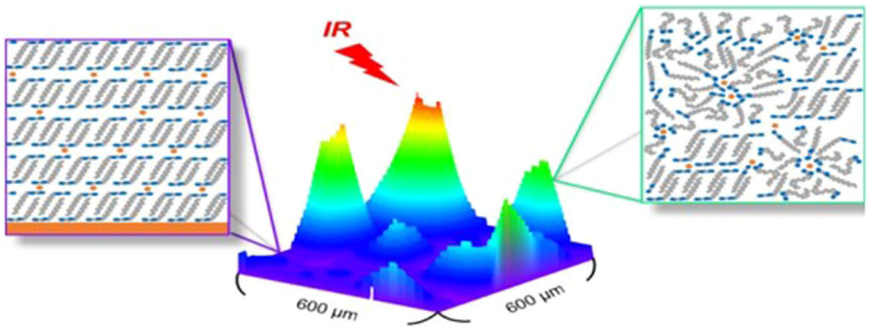

Fig. 11 | Schematic distribution of OLDA molecules on the Cu surface using IR microscopy. The temperature, adsorption time, and initial concentration of OLDA were 150 °C, 48 h, and 1 mM, respectively. Adapted from ref. 53 with permission from American Chemical Society© 2022.

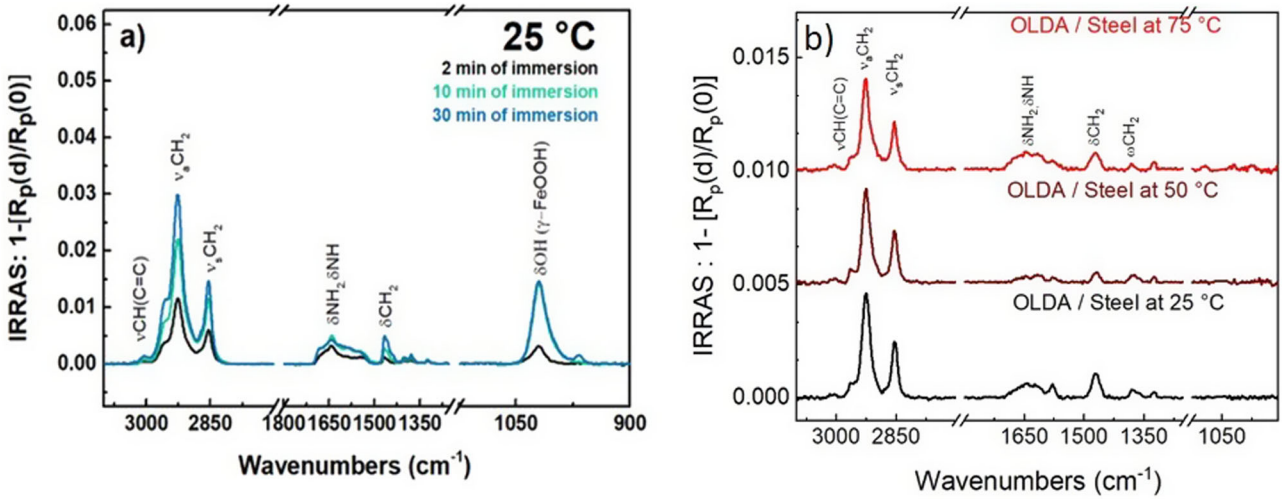

Fig. 12 | Influence of the corrosive medium/immersion time/temperature on the OLDA layer structure and thickness. a Ex situ IRRAS spectra of OLDA barrier formed onto the carbon steel for 2 min, 10 min and 30 min of immersion at 25 °C into a 100 mg kg^{-1} OLDA/200 mg kg^{-1} NaCl solution (adapted from ref. 58 with permission from Elsevier© 2023). **b** Ex situ IRRAS spectra of the OLDA layer adsorbed onto the carbon steel surface after 80 min of immersion in a deaerated solution containing 100 mg kg^{-1} of OLDA at a $pH_{25°C}$ = 11.0 for three temperatures 25 °C, 50 °C and 75 °C (adapted from ref. 47 under the CC BY license© 2024).

and 75 °C (Fig. 12b)[47]. For the first case, when corrosion products were present on the surface (active corrosion), the OLDA layer thickness increased with immersion time (2–140 min) and temperature (25–50 °C) from 4 nm to 20 nm suggesting an accumulation of OLDA molecules on the surface and probably the formation of mixed layer OLDA/corrosion products. For the second case, when corrosion processes were strongly limited due to the water chemical conditioning, the OLDA layer thickness was estimated to be 1.6 nm, regardless of the temperature. This value was comparable with those found for OLDA layers formed on inert surfaces such as gold[58] suggesting the formation of a monolayer in the absence of corrosion products.

The compactness of FFA layers and the influence of oxides have been minimally explored in the literature. In 1968, Bascom[67], using contact angle measurements (performed with organic solvents), have noted a difference in the compactness of ODA molecules depending on the nature of the substrate. For preoxidized steel surfaces up to 200 °C, the compactness of the ODA films decreased with increasing temperature. For temperatures above 200 °C, the compactness of the films increased. In 1998, Lee[24] have studied the structure of an LB film of ODA deposited on glass at different surface pressures and transfer rate. It was found that for small surface pressures and high transferring rates, the arrangement of ODA molecules on glass may be nonordered and irregular. The film was thus nonuniform and hydrophilic. Recently, the OLDA layer structure was investigated during temperature variations from 25 °C to 75 °C by EIS measurements and PM-IRRAS analyses[68]. The alkyl chain of OLDA presents *gauche* defects which can be favourable for a disordered structure of the layer on the surface. EIS measurements revealed the same temperature dependence of the OLDA layer conductivity and the electrolyte resistance suggesting that the ions and water crossed the OLDA layer through structural defects.

Overall, the different studies showed some tendencies for the FFAs layer thickness and its compactness. The layer thickness was that of a monolayer on inert surfaces such as mica or gold and on the steel surface in the absence of corrosion products. On corrodible surfaces and in the presence of corrosion products, the layer thickness exceeds that of the monolayer and according to different authors, multilayers or mixed layers are formed. Therefore, it is important to consider the role of corrosion products when interpreting the thickness values of FFAs layers.

The link between the inhibition properties and the structural properties of FFAs barriers is a delicate but crucial point for the understanding and improving of this technology but it still remains ambiguous. Few studies have addressed the correlation between the structure of the barrier and the inhibition properties of amines. Trabanelli and Carassiti[69] and Braun et al.[70] have investigated the influence of carbon chain length on inhibition properties. A better inhibition efficiency was achieved by increasing the number of carbons on the aliphatic chain at identical molar concentrations. Nevertheless, beyond a critical number of carbon atoms, the inhibition efficiency decreased. Long carbon chains cause steric hindrance and thus disadvantage contact between amine groups and the metal surface.

Conclusions and future recommendations

This review summarized the current understanding of FFAs as effective inhibitors against generalized, localized, and erosion corrosion, particularly on carbon steel surfaces. It covered both academic and industrial research on FFAs, identifying gaps in knowledge that, if addressed, could enhance the understanding of FFAs. One of the main difficulties encountered in this domain is the characterization of organic nanometric layers adsorbed on rough and corrodible surfaces. Examples illustrated various research axes, the used analytical and surface techniques, the data they yield, and the conclusions drawn from them.

The FFAs performance depends on various physical and chemical parameters. Optimal concentrations for maximum protection often align with the CMC, yet discrepancies exist between theoretical or experimental values and current industrial injection concentrations. Temperature significantly affects FFAs solubility and thermal degradation, especially within the 120 °C to 275 °C range, impacting surface adsorption. Precise solubility values remain undocumented. Studies on thermal stability, decomposition products, and decomposition kinetics of FFAs are sparse. Kinetics of FFAs adsorption and desorption have not been well explored. Limited research has been focused on time-dependent adsorption and desorption, primarily addressing "labile" rather than directly adsorbed layers. Recent findings indicate immediate OLDA adsorption on carbon steel at high initial concentrations in solution, with rapid steady-state adsorption occurring under conditions limiting steel corrosion. A slower steady state is reached when corrosion products form concurrently with OLDA adsorption. Different adsorption mechanisms such as radical, physisorption/chemisorption and chelates/complexes formation have been proposed, but experimental validation of these mechanisms is rare. A consensus exists on preferential FFAs adsorption on oxides versus on bare metal surfaces. The barrier thickness depends on the surface, monolayers are formed on gold or mica, whereas multilayers are formed on steel in presence of corrosion products. ODA forms organized layers on gold and mica, while OLDA exhibits heterogeneous organization on copper and steel. Recent findings suggest that the OLDA layer may contain structural defects, allowing the electrolyte to penetrate the layer.

Crucial questions remain about the use of FFAs during both operation and shutdown, particularly concerning how physicochemical and thermodynamic parameters—such as concentration, solubility, pH, temperature, dissolved oxygen, duration, and aggressive ions—affect barrier formation. Understanding the link between structural properties and inhibition efficiency, and the effects of these parameters on barrier ageing, would be relevant. This involves desorption at various temperatures and under diverse conditions, and barrier stability in air in the presence of humidity and oxygen. Addressing these questions from an industrial standpoint would enable better anticorrosion treatment adaptations, enhancing FFAs adsorption (adsorption mechanisms), managing FFAs quantity and frequency injection (barrier thickness and adsorption/desorption kinetics), and improving the understanding of the barrier lifespan (barrier ageing). This approach could also support the development of other more effective inhibitors (link between structural properties and inhibition properties), contributing to a more sustainable water management in industrial systems. Achieving these goals require an integrated approach, combining and refining molecular dynamics simulations, analytical, surface, and electrochemical techniques while acknowledging their respective advantages and limitations.

Data availability

No datasets were generated or analysed during the current study.

Received: 25 July 2024; Accepted: 5 October 2024;
Published online: 01 November 2024

References

1. Fujii, S. & Aramaki, K. *Proceedings of the 1st European symposium on corrosion inhibitors* Ferrara, Italy (1960).
2. Betova, I., Bojinov, M. & Saario, T. Film-forming amines in steam/water cycles – structure, properties, and influence on corrosion. *Tech. Res. Cent. Finl.* **VTT-R-0323**, 1–41 (2014).
3. Patil, V. & Sastry, M. Formation of close-packed silver nanoparticle multilayers from electrostatically grown octadecylamine/colloid nanocomposite precursors. *Langmuir* **16**, 2207–2212 (2000).
4. IAPWS. Technical Guidance Document: Application of Film Forming Substances in Fossil and Combined Cycle Plants. **TGD8-16**, (2019).
5. Chernyshev, E. V. et al. Increasing the corrosion resistance of equipment due to the use of film-forming amines. *Power Technol. Eng.* **40**, 34–37 (2006).
6. Topp, H., Hater, W., De Bache, A. & zum Kolk, C. Film-forming amines in shell boilers. *PowerPl. Chem.* **14**, 38–48 (2012).
7. Ryzhenkov, A. V., Pogorelov, S. I., Kurshakov, A. V., Morozov, M. A. & Ryzhenkova, N. V. Prospects for the application of film-forming amines in power engineering. *Surf. Contact Mech. Tribol. XII* **91**, 127–137 (2015).
8. Wagner, R. & Czempik, E. Experience in preservation of the water steam cycle in CCPP (combined cycle power plants) with ODA (octadecylamine). *J. Energy Power Eng.* **10**, 32–38 (2016).
9. Rudolph, L., Fandrich, J. & Ramminger, U. CFD calculation method for the assessment of the impact of film-forming amines on local deposition at the tube sheet of steam generators. *NPC International Conference*, Brighton, United Kingdom (2016).
10. Smith, B. et al. Determination of oleyl propylenediamine, a commonly used film forming amine powerplant chemistry. *Power Technol. Eng.* **19**, 129–140 (2017).
11. Hater, W., Smith, B., Mccann, P. & De Bache, A. Experience with the application of a film forming amine in the Connah's quay triple stage combined cycle gas turbine power plant operating in cycling mode. *PowerPl. Chem.* **20**, 136–144 (2018).
12. Hoenig, S. H. et al. Technoeconomic benefits of film-forming amine products applied to steam surface condensers. *PowerPl. Chem.* **23**, 4–16 (2021).
13. Rahman, M., Al-Hamzah, A., Al-Sahary, A., Fellows, C. M. & Al-Farsani, I. M. Film-forming amine product as an alternative to carbohydrazide oxygen scavenger in high pressure boilers. *Water Resour. Ind.* **29**, 100212 (2023).
14. Filippov, G. Experience in commissioning the secondary coolant circuit equipment of power unit No. 2 at the Armyanskaya nuclear power station after its preservation. *Teploenergetika* **45**, 42–44 (1998).
15. Odar, S. & Rudling, P. Use of film forming amines (FFA) in nuclear power plants for lay-up and power operation. *ANT International* 1–20 (2017).
16. Ramminger, U. & Hoffmann-Wankerl, S. The application of film-forming amines in secondary side chemistry treatment of NPPs. *NPC International Conference*, Paris, France (2012).
17. Ramminger, U. et al. Qualification of FFA treatment for the water-steam cycle as an innovative lay-up strategy for the long-term outage of a CANDU-6 reactor. *NPC International Conference*, Sapporo, Japan (2014).
18. Hasan, M., Montashirur Rahman, M., Kabir, A., Apblett, A. & Foutch, G. L. Mass-transfer coefficient as an indicator of resin performance: impacts of film-forming amines and storage time on condensate polishing ion-exchange resins. *Ind. Eng. Chem. Res.* **57**, 10601–10608 (2018).
19. Tyapkov, V. F. & Kharitonova, N. L. Applying film-forming amines for rendering corrosion resistance to structural materials of equipment and piping of power units at nuclear power plants (NPP) (Review). *Therm. Eng.* **69**, 653–661 (2022).
20. Stiller, K., Witting, T. & Urschey, M. The analysis of film-forming amines-Methods, possibilities, limits and recommendations. *Power Technol. Eng.* **13**, 602–610 (2011).
21. Lendi, M. Continuous photometric determination of film-forming amines. *Powerpl. Chem.* **17**, 1–5 (2015).

22. Jjunju, F. P. M. et al. Screening and quantification of aliphatic primary alkyl corrosion inhibitor amines in water samples by paper spray mass spectrometry. *Anal. Chem.* **88**, 1391–1400 (2016).
23. Brunner, A. M. et al. Liquid chromatography-high-resolution mass spectrometry-based target and nontarget screening methods to characterize film- forming amine-treated steam-water systems. *Ind. Eng. Chem. Res.* **59**, 22301–22309 (2020).
24. Lee, Y. L. Surface characterization of octadecylamine films prepared by Langmuir-Blodgett and vacuum deposition methods by dynamic contact angle measurements. *Langmuir* **15**, 1796–1801 (1999).
25. Petrova, T. I., Dyachenko, F. V. & Orlov, K. A. National and international guidelines for the use of reagents containing film-forming amines for the organization of TPP water chemistry regime. *Therm. Eng.* **65**, 222–225 (2018).
26. Lee, Y., Hur, D. H., Lee, J. & Jeon, S. Effect of film forming amine on magnetite deposition behaviors of alloy 690TT tube in secondary water condition. *Transactions of the Korean Nuclear Society* (2021).
27. Malik, M. A., Hashim, M. A., Nabi, F., AL-Thabaiti, S. A. & Khan, Z. Anti-corrosion ability of surfactants: a review. *Int. J. Electrochem. Sci.* **6**, 1927–1948 (2011).
28. Bohnsack, G. Korrosionsinhibierung durch das im Helaminenthaltene'filmbildende'Amin. *VGB KraftwerksTechnik*, **77** (1997).
29. Mao, F., Dong, C. & Macdonald, D. D. Effect of octadecylamine on the corrosion behavior of Type 316SS in acetate buffer. *Corros. Sci.* **98**, 192–200 (2015).
30. Duprat, M., Dabosi, F., Moran, F. & Rocher, S. Inhibition of corrosion of a carbon steel by the aliphatic fatty polyamines in association with organic phosphorous compounds in 3% sodium chloride solutions. *Corrosion* **37**, 262–266 (1981).
31. Rohani-Rad, A., Mofidi, J. & Modaress-Tehrani, Z. Anticorrosive behaviour of octadecylamine for protection of boiler surfaces. *Corr. Eng. Sci. Technol.* **38**, 79–80 (2003).
32. Pensini, E., Van Lier, R., Cuoq, F., Hater, W. & Halthur, T. Enhanced corrosion resistance of metal surfaces by film forming amines: A comparative study between cyclohexanamine and 2-(diethylamino) ethanolbased formulations. *Water Resour. Ind.* **20**, 93–106 (2018).
33. Ma, Y. et al. Understanding the anticorrosive mechanism of a cross-linked supramolecular polymer for mild steel in the condensate water: comprehensive experimental, molecular docking, and molecular dynamics investigations. *J. Mol. Model.* **26**, 1–17 (2020).
34. Bäßler, R., Uhlemann, M. & Mummert, K. Inhibiting effect of octadecylamine on pitting corrosion behaviour of stainless steel type 1.4541 up to 250 °C. *Mater. Corros.* **50**, 146–153 (1999).
35. Banica, C. E., Czempik, E., Vogt, C. & Schneider, F. Influence of hot water conditioning on the corrosion behavior of carbon steel. *Mater. Corr.* **53**, 256–263 (2002).
36. Lee, Y.-B., Jeon, S.-H., Bae, B. J., Hur, D. H. & Lee, J. H. Effect of organic film on magnetite deposition behavior of alloy 690 steam generator tubes in simulated PWR secondary system. *J. Mater. Res. Technol.* **20**, 2527–2541 (2022).
37. De Seranno, T. et al. Effect of film-forming amines on the acidic stress-corrosion cracking resistance of steam turbine steel. *Metals* **10**, 1–20 (2020).
38. Weerakul, S., Leaukosol, N., Lister, D. H., Mori, S. & Hater, W. Effects on flow-accelerated corrosion of oleylpropanediamine under single-phase water conditions pertinent to power plant feedwater. *Corrosion* **76**, 217–230 (2020).
39. Ge, H.-H., Zhou, G.-D., Liao, Q.-Q., Lee, Y. G. & Loo, B. H. A study of anti-corrosion behavior of octadecylamine-treated iron samples. *Appl. Surf. Sci.* **156**, 39–46 (2000).
40. Bommersbach, P., Alemany-Dumont, C., Millet, J. P. & Normand, B. Formation and behaviour study of an environment-friendly corrosion inhibitor by electrochemical methods. *Electrochim. Acta* **51**, 1076–1084 (2005).
41. Jäppinen, E. et al. Corrosion behavior of carbon steel coated with octadecylamine in the secondary circuit of a pressurized water reactor. *J. Mater. Eng. Perform.* **26**, 6037–6046 (2017).
42. Baux, J. et al. Film-forming amines for the corrosion protection of carbon steels in nuclear power plant secondary circuit conditions: an impedance study. *J. Electrochem. Soc.* **167**, 061504 (2020).
43. Cuoq, F., Benguigui, J., Geijselaers, C. & Lampert, F. Linking thermoelectric effect and adsorption of film forming amine as a corrosion inhibitor for industrial systems. *Ind. Eng. Chem. Res.* **59**, 8492–8495 (2020).
44. Kuilya, S., Subramanian, V., Bera, S. & Rangarajan, S. Evaluation of octadecylamine for the corrosion inhibition of Incoloy 800. *Corr. Eng. Sci. Technol.* **56**, 119–128 (2021).
45. Cao, S., Hu, J., Xie, J., Liang, Q. & Yin, L. Research on the film-forming characteristics of octadecylamine at high temperatures,. *Anti Corr. Methods Mater.* **60**, 14–19 (2013).
46. Vidojkovic, S., Mijajlovic, M., Lindeboom, R. E. F. & Jovicic, V. Thermal stability of film forming amines-based corrosion inhibitors in high temperature power plant water solutions. *Energy Sci. Eng.* **12**, 304–328 (2024).
47. Jero, D. et al. Adsorption kinetics and inhibition mechanisms of a film-forming amine on carbon steel surfaces. *Electrochim. Acta* **498**, 144625 (2024).
48. Zhu, Y., Free, M. L., Woollam, R. & Durnie, W. A review of surfactants as corrosion inhibitors and associated modeling. *Prog. Mat. Sci.* **90**, 159–223 (2017).
49. Kumar, A. et al. Investigation into the interaction between surface-bound alkylamines and gold nanoparticles. *Langmuir* **19**, 6277–6282 (2003).
50. Khodyrev, B. N., Krichevtsov, A. L. & Sokolyuk, A. A. Studying the processes relating to oxidation of organic substances contained in the coolant of thermal and nuclear power stations. *Therm. Eng.* **57**, 553–559 (2010).
51. Fan, B. et al. Revealing the assembly mechanism of an octadecylamine based supramolecular complex on mild steel in condensate water: correlative experimental and theoretical studies. *J. Mol. Liq.* **292**, 111446 (2019).
52. Jiang, B., Sun, W., Cai, J., Chen, S. & Hou, B. Inhibition of carbon steel corrosion in HCl solution using N-oleyl-1,3-propanediamine based formulation. *Colloids Surf. A Physicochem. Eng. Asp.* **624**, 126824 (2021).
53. Yoshioka, H. et al. Microscopic structure and binding mechanism of the corrosion-protective film of oleylpropanediamine on copper in hot water. *J. Phys. Chem. C.* **126**, 6436–6447 (2022).
54. Genxian, L. et al. Adsorption behaviour of film-forming amine on pre-oxidized carbon steel surface. *Nucl. Eng. Technol.* **54**, 1185–1194 (2022).
55. Liu, C. et al. Effect of octadecylamine concentration on adsorption on carbon steel surface. *Nucl. Eng. Technol.* **52**, 2394–2401 (2020).
56. Liu, Z., Lv, B., Wu, D. & Sun, Y. Morphology and magnetic properties of α-Fe_2O_3 particles prepared by octadecylamine-assisted hydrothermal method. *Particuology* **10**, 456–461 (2012).
57. Jack, M. et al. The interaction of a film-forming amine with surfaces of a recirculating experimental water loop. *Proc. Int. Conf. Heat Exch. Fouling Clean*. 112–118 (2015).
58. Jero, D. et al. Film-forming amines adsorption and corrosion kinetics on carbon steel surface in neutral solution investigated by EIS and PM-IRRAS analysis. *Electrochim. Acta* **443**, 141925 (2023).
59. Takahashi, M., Kobayashi, K., Takaoka, K. & Tajima, K. Structural characterization of an octadecylamine Langmuir-Blodgett film adsorbed with methyl orange. *J. Colloid Interface Sci.* **203**, 311–316 (1998).
60. Dai, S., Zhang, X., Du, Z., Huang, Y. & Dang, H. Structural properties and Raman spectroscopy of lipid Langmuir monolayers at the air-water interface. *Colloids Surf. B* **42**, 21–28 (2005).
61. Patil, K. G., Santhanam, V., Biswas, S. K. & Ayappa, K. G. Combined atomic force microscopy and modeling study of the evolution of

octadecylamine films on a mica surface. *J. Phys. Chem. C* **114**, 3549–3559 (2010).
62. Oviedo, J., San-Miguel, M. A., Heredia-Guerrero, J. A. & Benítez, J. J. Electrostatic induced molecular tilting in self-assembled monolayers of n-octadecylamine on mica. *J. Phys. Chem. C* **116**, 7099–7105 (2012).
63. Campen, S., Green, J. H., Lamb, G. D. & Spikes, H. A. In situ study of model organic friction modifiers using liquid cell AFM: Self-assembly of octadecylamine. *Tribol. Lett.* **58**, 1–15 (2015).
64. Abu Tahari, M. N., Hakim, A., Wan Isahak, W. N. R., Samad, W. Z. & Yarmo, M. A. Adsorption of CO_2 on Octadecylamine-impregnated on SiO_2: physical and chemical interaction studies. *Adv. Mat. Res.* **1087**, 137–141 (2015).
65. Baux, J. et al. Impedance analysis of film-forming amines for the corrosion protection of a carbon steel. *Electrochim. Acta* **283**, 699–707 (2018).
66. Liao, Q. Q., Zhou, G. D., Ge, H. H. & Qi, L. M. Characterisation of surface film on iron samples treated with octadecylamine. *Corr. Eng. Sci. Technol.* **42**, 102–105 (2007).
67. Bascom, W. D. The wettability of n-octadecylamine, n-octadecyl alcohol and n-octadecanoic acid films adsorbed on thermally treated metal oxide surfaces. *J. Colloid Interface Sci.* **26**, 89–94 (1968).
68. Jero, D. et al. Analysis of a film-forming amine response in impedance spectra. *Electrochim. Acta* **498**, 144690 (2024).
69. Trabanelli, G. & Carassiti, V. Mechanism and phenomenology of organic inhibitors. *Adv. Corr. Sci. Technol.* **147**, 228 (1970).
70. Braun, R. D., Lopez, E. E. & Vollmer, D. P. Low molecular weight straight-chain amines as corrosion inhibitors. *Corros. Sci.* **34**, 1251–1257 (1993).
71. Kuang, W., Mathews, J. A., Taylor, M. L. & Macdonald, D. D. The effect of Anodamine on the corrosion behavior of 1018 mild steel in deionized water: II. electrochemical impedance analysis. *Electrochim. Acta* **136**, 493–503 (2014).

Acknowledgements

This work was carried out with the financial support of ODYSSEE Environment. The authors gratefully acknowledge the partners of the project: Fabrice Chaussec and Amaury Buvignier from ODYSSEE Environnement as well as Marion Roy from CEA Saclay.

Author contributions

D.J.: conceptualization, data curation, formal analysis, investigation, methodology, writing - original draft. N.C. and N.P.: conceptualization, formal analysis, investigation, methodology, project administration, supervision, validation, writing - review & editing. All authors read and approved the final manuscript.

Competing interests

The authors declare no competing interests.

Additional information

Correspondence and requests for materials should be addressed to Deni Jero, Nicolas Caussé or Nadine Pébère.